Chemistry and Physics of Lipids xxx (2010) xxx–xxx

Contents lists available at ScienceDirect

Chemistry and Physics of Lipids

journal homepage: www.elsevier.com/locate/chemphyslip

Phase state and surface topography of palmitoyl-ceramide monolayers

Maria Laura Fanani*, Bruno Maggio

Departamento de Química Biológica, Centro de Investigaciones en Química Biológica de Córdoba (CIQUIBIC), Facultad de Ciencias Químicas, CONICET, Univ. Nacional de Córdoba, Haya de la Torre y Medina Allende, Ciudad Universitaria, X5000HUA, Córdoba, Argentina

ARTICLE INFO

Article history:
Received 18 February 2010
Received in revised form 15 April 2010
Accepted 16 April 2010
Available online xxx

Keywords:
Sphingolipids
Lipid domains
Brewster Angle Microscopy
Isobars
Phase diagram
Monolayer thickness

ABSTRACT

In cell biology (and in many biophysical) studies there is a natural tendency to consider ceramide as a highly condensed, solid-type lipid conferring rigidity and close packing to biomembranes. In the present work we advanced the understanding of the phase behavior of palmitoyl-ceramide restricted to a planar interface using Langmuir monolayers under strictly controlled and known surface packing conditions. Surface pressure–molecular area isotherms were complemented with molecular area–temperature isobars and with observations of the surface topography by Brewster Angle Microscopy. The results described herein indicate that palmitoyl-ceramide can exhibit expanded, as well as condensed phase states. Formation of three phases was found, depending on the surface pressure and temperature: a solid (1.80 nm thick), a liquid-condensed (1.73 nm thick, likely tilted) and a liquid-expanded (1.54 nm thick) phase over the temperature range 5–62 °C. A large hysteretic behavior is observed for the S phase monolayer that may indicate high resistance to domain boundary deformation. A second (or higher) order S → LC phase transition is observed at about room temperature while a first order LC → LE transition occurs in a range of temperature encompassing the physiological one (observed above 30 °C at low surface pressure). This phase behavior broadens the view of ceramide as a type of lipid not-always-rigid but able to exhibit polymorphic properties.

1. Introduction

Since when it was proposed as a key player in various cell signaling processes (Kolesnick et al., 2000), ceramide (Cer) has received considerable attention and it became increasingly clear that most of its effects are strongly related to its capacity to markedly influence the physical properties of cell membranes (van Blitterswijk et al., 2003; Goni and Alonso, 2009). The generation of Cer upon sphingomyelin enzymatic breakdown induces highly ordered segregated lateral structures in artificial systems and other membrane changes (Lopez-Montero et al., 2009; Fanani et al., 2010) that may be involved in the structural dynamics related to cell membrane signaling (Grassme et al., 2007).

Sphingomyelin is the major sphingolipid present in the outer leaflet of cell plasma membranes (Venien and Le, 1988), its fatty acid composition consisting mostly in saturated fatty acids. C16:0 is one of the fatty acids that comprise the bulk of the fatty acid pool linked to sphingomyelin isolated from natural sources (Estep et al., 1979). Therefore, sphingomyelinase-generated Cer in the plasma membrane contains the same fatty acid composition and will predominantly consist of palmitoylCer (pCer) (Goni and Alonso, 2006). The physical properties of Cer and its interaction with phospholipids, cholesterol and/or sphingomyelin have been studied in binary and ternary model system (Maggio et al., 1978; Goni and Alonso, 2006; Lopez-Montero et al., 2009). Regarding pCer, an increasing amount of information is published on the effects of this lipid in binary mixtures (Holopainen et al., 2000, 2001; Goni and Alonso, 2006; Goni and Alonso, 2009; Busto et al., 2009; Lopez-Montero et al., 2009; Karttunen et al., 2009) but comparatively little work has dealt with the physical properties of pure pCer itself (Shah et al., 1995; Chen et al., 2000), likely because technical difficulties have been reported for reaching workable homogeneous samples at proportions of pCer above 30 mol% (Holopainen et al., 2000; Busto et al., 2009), a situation also found for bovine brain Cer (Carrer and Maggio, 1999). An in-depth calorimetric and structural (X-ray diffraction) study was published by Shah et al. (1995). A complex thermotropic behavior was observed for the fully hydrated pCer. A metastable bilayer gel phase exists at low temperatures, with increasing temperature an exothermic transition occurs at 64 °C to form a stable bilayer probably chain tilted with respect to the bilayer normal. Further increase in temperature leads to a disordered (likely HII-type) chain-melted phase (T_m 90 °C). These results were further supported by Moore's work

Abbreviations: pCer, N-palmitoylsphingosine; LE, liquid-expanded; LC, liquid-condensed; S, solid; BAM, Brewster Angle Microscopy; HII, hexagonal II phase; C_s^{-1}, compressibility modulus.

* Corresponding author. Tel.: +54 351 4334168; fax: +54 351 4334074.
E-mail address: lfanani@fcq.unc.edu.ar (M.L. Fanani).

0009-3084/$ – see front matter © 2010 Elsevier Ireland Ltd. All rights reserved.
doi:10.1016/j.chemphyslip.2010.04.008

using infrared studies (Chen et al., 2000). In a recent study of pCer/palmitoylsphingomyelin interactions in monolayers it was mentioned that pure pCer monolayers exhibit an isothermal surface pressure-induced condensed–condensed phase transition at room temperature (Busto et al., 2009). That transition occurs about 40 °C below the gel–gel transition observed for bulk aqueous dispersions of pCer (Shah et al., 1995; Chen et al., 2000). In cell biology (and in many biophysical) studies there is a traditional tendency to consider Cer as a highly condensed, solid-type, lipid conferring rigidity and close packing to biomembranes. In the present work we advanced the understanding of the phase behavior of pCer restricted to a planar interface using Langmuir monolayers under strictly controlled and known surface packing conditions. This avoids relaxation of lateral tensions causing escape to third dimension through formation of non-lamellar phases that is possible in bulk systems (Veiga et al., 1999). Surface pressure–molecular area isotherms were complemented with molecular area–temperature isobars and with observations of the surface topography by Brewster Angle Microscopy (BAM). The results indicate that, similar to other lipids [including other sphingolipids (Maggio et al., 2004)], pCer can exhibit expanded, as well as condensed phase states. Formation of three phases was found, depending on the surface pressure and temperature: a solid, a liquid-condensed and a liquid-expanded phase over the temperature range 5–62 °C. Noteworthy, a liquid-expanded–condensed transition occurs in a range of temperature encompassing the physiological one (34–39 °C).

2. Experimental procedures

2.1. Chemicals

Palmitoyl-ceramide (pCer) was purchased from Avanti Polar Lipids (Alabaster, AL), it was over 99% pure by thin-layer chromatography and was used without further purification. Solvents and chemicals were of the highest commercial purity available. The water was purified by a Milli-Q (Millipore, Billerica, MA) system, to yield a product with a resistivity of ~18.5 MU/cm. Absence of surface-active impurities was routinely checked as described elsewhere (Bianco and Maggio, 1989). The lipid stock solution was kept at −70 °C until use and at −20 °C during the working day.

2.2. Monolayer isotherms and isobars

Compression–expansion isotherms and isobars were obtained for synthetic pCer at different temperatures and surface pressures. Typically, lipid monolayers were spread from 25 μl of chloroform solution onto a 266 cm^2 Teflon trough filled with 200 mL of 145 mM NaCl, pH ~5.6. The film was relaxed for 5 min at 0 mN/m and subsequently compressed to the target pressure. Surface pressure and film area were continuously measured and recorded with a KSV Minitrough equipment (KSV, Helsinski, Finland) enclosed in an acrylic box. Subphase temperature was controlled by a Haake bath with external circulation (Thermo Electron, Karlsruhe, Germany) and automatically recorded (Lab-Trax, World Precision Instruments, Sarasota, FL) as a function of time. When second compression of the film was studied, the lipid monolayer was compressed up to 35 mN/m, relaxed by decompression to 0.7 mN/m (in about 5 min), allowed to stand at that pressure for 5 min and subsequently compressed to collapse. The collapse and other phase transition points were estimated by the third derivate method (Brockman et al., 1980). Compressibility modulus (C_s^{-1}) was calculated from the isotherm data as: $C_s^{-1} = -A(d\pi/dA)_T$ (Ali et al., 1991; Mohwald, 1995). After reaching the target pressure, isobars were recorded 5 min at 5 °C and then heated to 62 °C (final temperature) at a rate of 1 °C/min. Isobaric thermal expansivity was calculated from isobar data as follows: $\lambda = (1/A)(dA/dT)_\pi$ (Mohwald, 1995). All measurements were performed at a compression rate of 1 ± 0.5 Å^2/mol/min and under N_2 atmosphere.

2.3. BAM measurements

Monolayers were prepared as described above but using a conveniently small Model 102 M equipment (NIMA Technology Ltd, Coventry, England). The Langmuir equipment was mounted on the stage of a Nanofilm EP3 Imaging Elipsometer (Accurion, Goettingen, Germany) used in the Brewster Angle Microscopy (BAM) mode. Zero reflection was set with a polarized 532λ laser incident on the bare aqueous surfaces at the Brewster angle (53.1°). After monolayer formation, and/or compression, the reflected light was collected with a 10× objective and a reflectivity index calculated [typically $R = (\text{grey level} - 13.3) \times 2.8e - 8$]. Assuming a refraction index of 1.33 and 1.5 for the aqueous surface and the lipid film respectively, R relates to the thickness (d) of the monolayer as follows: $R = 0.07784\,(-3.416e - 3 \times d)^2$ (Lheveder et al., 2000).

3. Results and discussion

Surface pressure–mean molecular area isotherms of pure pCer were performed at different temperatures. At room temperature, the isotherms apparently show a transition-free condensed behavior as previously reported (Holopainen et al., 2001; Busto et al., 2009). However a diffuse, probably second or higher order, phase transition between two condensed phases that usually goes unnoticed can be detected as an inflection in the isotherm curve and compressibility modulus (C_s^{-1}) analysis (Fig. 1, see black arrows). The existence of this transition was mentioned in a recent publication when the abscissa axis was considerably expanded (Busto et al., 2009). At temperatures 22–27 °C, the phase present at low surface pressures was characterized by a C_s^{-1} value of about 300–500 mN/m and the phase present at high surface pressures shows C_s^{-1} values of about 600–800 mN/m. According with the C_s^{-1} values observed, these phases can be characterized as liquid-condensed (LC) and solid (S), respectively (Davies and Rideal, 1963). These C_s^{-1} values agree with published data (Holopainen et al., 2001) where a biphasic behavior of C_s^{-1} was reported but without discussion. It is worth noting that the C_s^{-1} values for the S phase of pCer found here are similar to those of the solid phase state of fatty acids and cholesterol (Davies and Rideal, 1963; Smaby et al., 1997) and are higher than the C_s^{-1} values reported for other phospholipids or sphingolipids with the only exception of galactosylceramide with saturated fatty acyl chains (Smaby et al., 1996). By contrast, the C_s^{-1} values found for the LC phase of pCer is rather similar to that reported for natural Cer (Maggio, 2004) and Cer-1 phosphate (Kooijman et al., 2009). Further features of this diffuse phase transition are provided by isobars analysis (see below).

At 45 °C and above, a first order liquid-expanded (LE)–LC phase transition is observed (see gray arrows in Fig. 1) involving a large change in molecular area (77% increase at 10 mN/m) (see also Fig. 5). This phase shows C_s^{-1} values of ≈60 mN/m, corresponding to a LE character (Davies and Rideal, 1963; Smaby et al., 1996). The presence of a LE phase for Cer was previously reported only for N-stearoyl Cer at 5.7 mN/m at 52 °C (Fidelio et al., 1986). This is not very different from what we found for pCer (at 11 mN/m at 49 °C, see Fig. 1). The difference observed indicates, as would be expected, that the addition of two methylene groups to the N-fatty acid substituent of Cer favors stabilization of the LC phase.

The isotherms for pCer at relatively low temperatures show a less condensed behavior during the first compression and become

Please cite this article in press as: Fanani, M.L., Maggio, B., Phase state and surface topography of palmitoyl-ceramide monolayers. Chem. Phys. Lipids (2010), doi:10.1016/j.chemphyslip.2010.04.008

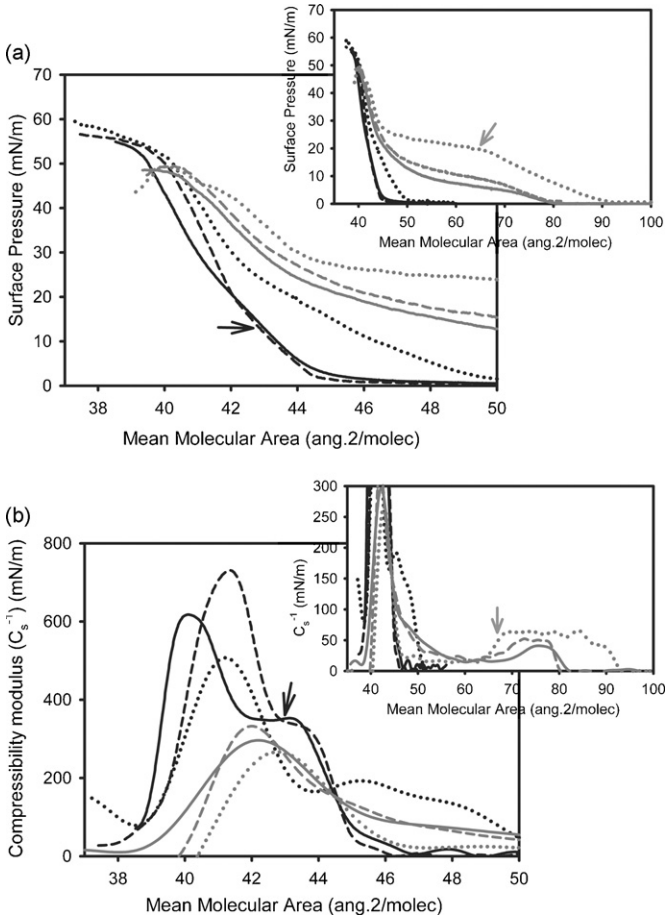

Fig. 1. First compression isotherms of pCer monolayers at different temperatures. Surface pressure (a) and compressibility modulus (C_s^{-1}) (b) mean molecular area curves are shown for pCer at 23 °C (black full line), 34 °C (black dashed line), 39 °C (black dotted line), 45 °C (gray full line), 49 °C (gray dashed line) and 62 °C (gray dotted line). The insets show an extended mean molecular area axis. Black arrows show the liquid-condensed–solid phase transition. Gray arrows show the beginning of the liquid-expanded–liquid-condensed phase transition. The curves show a single representative experiment from a set of triplicates.

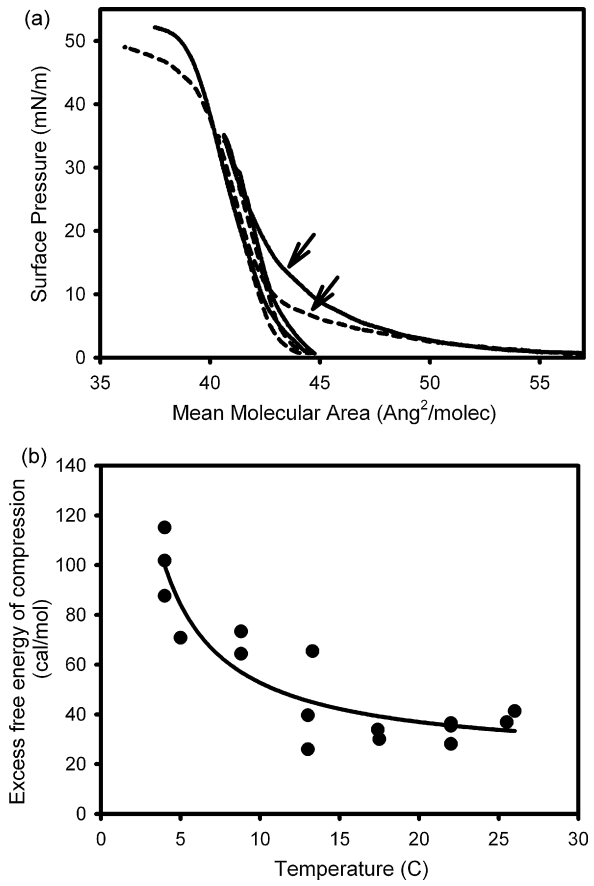

Fig. 2. Hysteretic behavior of pCer at low temperatures. (a) Compression cycles of pCer monolayers at 4 °C (full line) and 13 °C (dashed line). The arrows indicate the first compression of the monolayers. At 35 mN/m the films were relaxed to 0.7 mN/m and recompressed to collapse. The curves show a single representative experiment from a set of duplicates/triplicates. (b) Excess free energy of compression calculated from the difference in the area integrated for the first and second compression curves over the interval 0.7–35 mN/m. Each point represents a single experiment. The full line represents the inverse first order fitting of the data.

more condensed during the second compression after expansion (Fig. 2a). This phenomenon implies a considerable hysteresis in the pCer monolayer, involving irreversible consumption of cohesion work, which is reduced with increasing temperature (Fig. 2b). It appears that, once pCer molecules are forced to closely pack and acquire the more condensed state, the intermolecular arrangement is quite irreversible under expansion (or, at least, its relaxation kinetics is much slower than the film expansion process). As reasonably expected, the increase of molecular thermal energy caused by increasing temperature leads to more favorable (or faster) reversibility.

Brewster Angle Microscopy (BAM) analysis of pCer monolayers at low temperatures shows coexistence of gas–solid phase (Fig. 3b–d). The pressure range for that phase coexistence correlates with the pressure range hysteretic behavior is apparent between the first and second compressions of the film. At high surface pressures, where a topographically uniform film is observed by BAM (Fig. 3e), the first and second compression curves became parallel (Fig. 2). This indicates that physical phenomena involved in the hysteretic behavior of pCer films at low temperatures may be related to the work of deformation of solid domain boundaries and to expulsion/condensation of the gas phase which is necessary for reaching a uniform film. This process involves energy values that reach ≈100 cal/mol at 5 °C (Fig. 2b). After the surface topography becomes homogeneous, the intermolecular organization is more stable under expansion-recompression.

We further analyzed the second compression of pCer monolayers at low temperatures, where the film shows uniform characteristics by BAM imaging at surface pressures above 0.7 mN/m. Below 20 °C, isotherms show a behavior with C_s^{-1} values that correspond to solid (S) phase over the whole range of surface pressure, likely with some diffuse transition between condensed states (Fig. 4). At about room temperature the LC–S phase transition observed for the first compression of pCer films (Fig. 1) becomes again evident in the surface pressure–area curve and the C_s^{-1} analysis from the second compression (Fig. 4, see arrow).

To further ascertain the phase behavior of pCer monolayers observed from isotherms we also performed isobars. After formation of the monolayer over a subphase at 4 °C and compressed to the desired surface pressure, the monolayer was heated while automatically keeping the surface pressure constant and allowing the film to expand (Fig. 5). At 10 and 20 mN/m smooth increases of mean molecular area was observed until reaching about 45–47 °C where a large increase of area occurs over a narrow temperature range (Fig. 5, see gray arrows). This phenomenon occurs in the temperature range for the LC–LE phase transition observed in the surface pressure-area isotherms (see also Fig. 7). The area change at 10 mN/m was characterized by two reproducible steps that are also evident from the isobaric thermal expansivity analysis (see

Please cite this article in press as: Fanani, M.L., Maggio, B., Phase state and surface topography of palmitoyl-ceramide monolayers. Chem. Phys. Lipids (2010), doi:10.1016/j.chemphyslip.2010.04.008

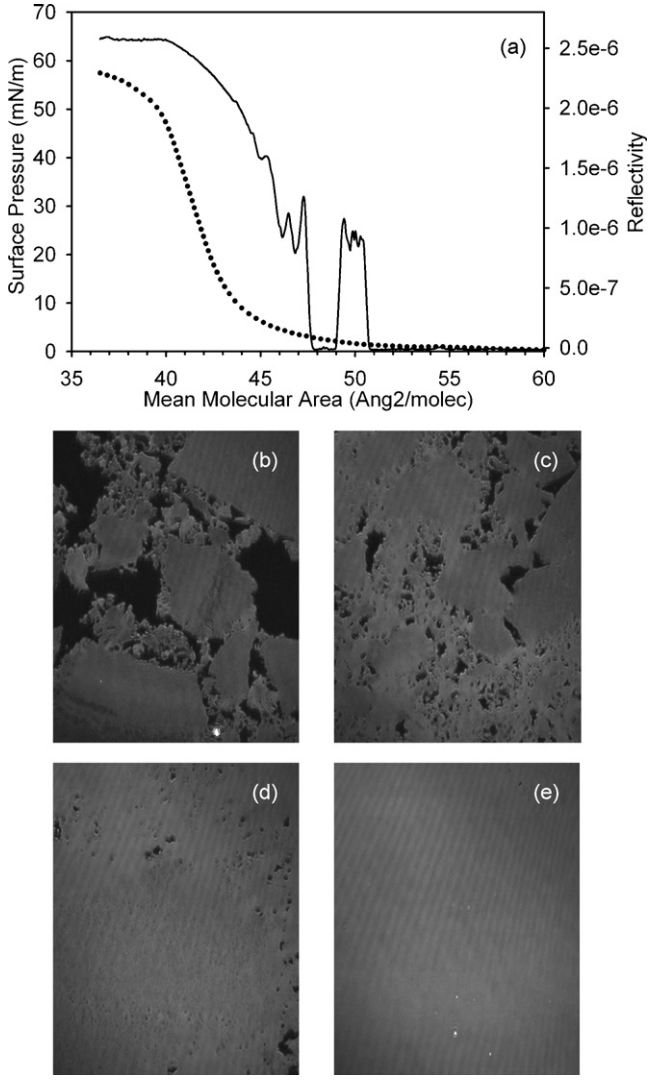

Fig. 3. BAM images of pCer monolayers reveal gas–liquid-condensed phase coexistence that explains hysteresis. (a) Continuous measurement of reflectivity (full line) and simultaneous compression isotherm curve (dotted line) at 15.6 °C. The noise of the reflectivity values observed at mean molecular areas larger than 44 Å^2/mol is a consequence of the average measurement of optical intensity in images with gas–solid phase coexistence (see panels b–d). (b–e) BAM images of pCer monolayers at 3.3 mN/m (b), 5.4 mN/m (c), 8.0 mN/m (d) and 16.7 mN/m (e) respectively. Image size 372 μm × 466 μm. All data was taken from a single representative experiment.

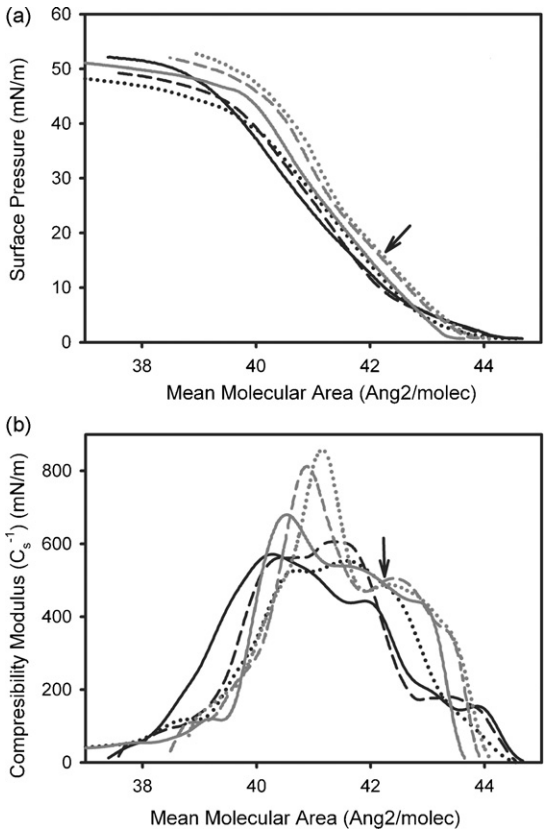

Fig. 4. Second compression isotherms of pCer monolayers at low temperatures. Surface pressure (a) and compressibility modulus C_s^{-1} (b) mean molecular area curves of recompression for pCer are shown at 4 °C (black full line), 9 °C (black dashed line), 13 °C (black dotted line), 17.5 °C (gray full line), 22 °C (gray dashed line) and 26 °C (gray dotted line). The monolayer was initially compressed to 35 mN/m and relaxed to 0.7 mN/m were a uniform film corresponding to a condensed phase is observed by BAM. After 5 min relaxation the second compression was registered. The arrows indicate the liquid-condensed–solid phase transition for pCer monolayers at 22 and 26 °C. The curves show a single representative experiment from a set of triplicates.

question mark in Fig. 5). We could not resolve if this indicates the existence of more than one expanded phase because it was not possible to explore area expansion at higher temperatures with our current technical set-up; no other indications on such change could be observed either by compression isotherms or by BAM studies. At surface pressures of 30 mN/m and above, isobars show a diffuse, but well defined and reproducible, change of slope at ≈20 °C that corresponds to the LC–S phase transition observed in the compression isotherms (see black arrows in Fig. 5).

To further characterize the topography of the three phases observed in the isotherm and isobar studies measurements of monolayer thickness (d) were performed by BAM (see Section 2). pCer monolayers at different temperatures show that the three surface phases described above have thickness values of 1.54 ± 0.04 (SEM), 1.73 ± 0.02 and 1.80 ± 0.02 nm for the LE, LC and S phases, respectively (see also Fig. 6). For this calculation a refraction index of 1.5 was assumed for the lipid film [taken from ellipsometric study of phospholipids (Ducharme et al., 1990)]. A previous study of BAM reflectivity of bovine brain Cer at 25 °C was reported but monolayer thickness was not calculated (Rosetti et al., 2003). In that work the isotherm reflected a condensed phase behavior and the reflectivity values were slightly lower than for the pCer reported here, also reflecting little dependence with surface pressure. For comparison, reported ellipsometric studies on phospholipid monolayers reveal thicknesses of approx. 1.5 nm for the LE phase and 2.2 nm for the completely untilted solid phase of DPPC (Ducharme et al., 1990).

The structural study in bulk dispersion of pCer reported by Shah et al. (1995) also described three phases: two lamellar bilayer gel phases and a chain-disordered phase at high temperature. The gel phase found at low temperature showed a periodicity of 4.7 nm between bilayers when fully hydrated and of 4.2 nm in the anhydrous state. In that article it was concluded that the 0.5 nm difference was due to the water layer. In the present study we can correlate such gel phase with the S phase observed at low temperatures in pCer monolayers. From our BAM measurements (thickness 1.80 ± 0.02 nm) a bilayer would correspond only to a thickness of 3.6 nm. The difference may be because the BAM technique is unable to evaluate the polar head group, with its associated hydrated shell, contribution to thickness in the pCer monolayer since this region has a reflection index rather similar to that of the aqueous subphase compared to that of the hydrocarbon region. Shah et al., also found a reduced periodicity (4.2 nm, including the water

Please cite this article in press as: Fanani, M.L., Maggio, B., Phase state and surface topography of palmitoyl-ceramide monolayers. Chem. Phys. Lipids (2010), doi:10.1016/j.chemphyslip.2010.04.008

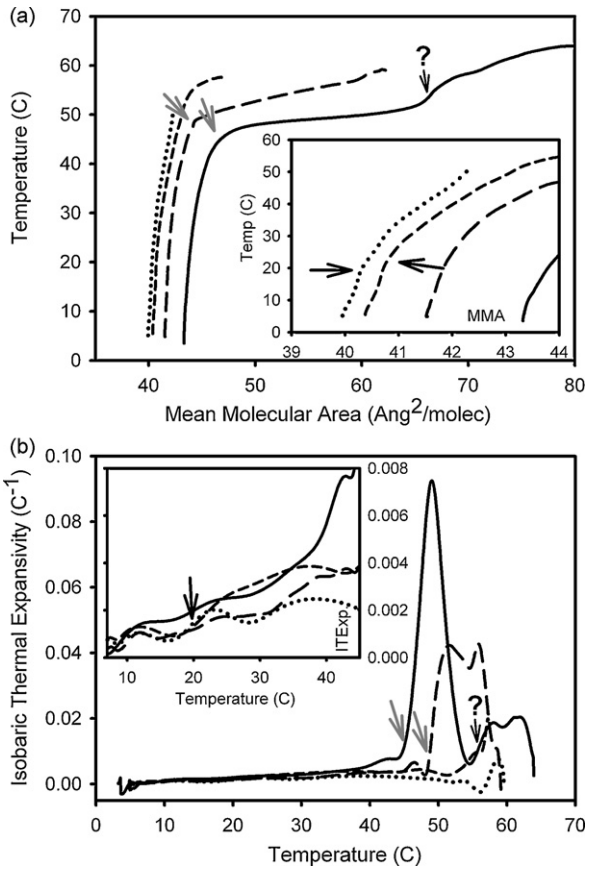

Fig. 5. Isobars of pCer monolayers at different surface pressures. Isobars (a) and isobaric thermal expansivity (b) of pCer monolayers at 10 mN/m (full line), 20 mN/m (long dashed line), 30 mN/m (short dashed line) and 37 mN/m (dotted line). To emphasize slope changes at about 20 °C for the latter two, the insets show an expanded mean molecular area axis. Gray arrows show the beginning of the liquid-condensed–liquid-expanded phase transition. Black arrows show the solid–liquid-condensed phase transition. The question marks indicate the transition to a putative second expanded phase. The curves show a single representative experiment from a set of triplicates.

layer) between bilayers of the gel phase at intermediate temperatures (Shah et al., 1995). This can be compared to the thickness of the LC phase found in our work with a monolayer thickness of 1.73 ± 0.02 nm which would make a 3.4 nm bilayer, considering only the hydrocarbon region. This second bulk gel phase was proposed to be tilted from measurements of inter-chain spacing or presenting a thinner water layer. Since our measurements by BAM do not include the polar head group orientation or hydration, our results indicating a thinner LC phase strengthen the hypothesis for the existence of a chain-tilted crystalline pCer phase both in bilayer and monolayer systems. Finally, a chain-melted phase was also reported by Shah et al. with a periodicity of 3.0 nm. The structure of this phase, whether bilayer or HII, was undefined in that work (Shah et al., 1995), nevertheless, a considerable amount of evidence underlines the capacity of Cer to favor formation of negatively curved topologies such as the HII-type (Veiga et al., 1999; Goni and Alonso, 2006). Our measurement of the LE phase thickness (1.54 ± 0.04 nm) may account for a 3.1 nm bilayer, excluding the polar head group.

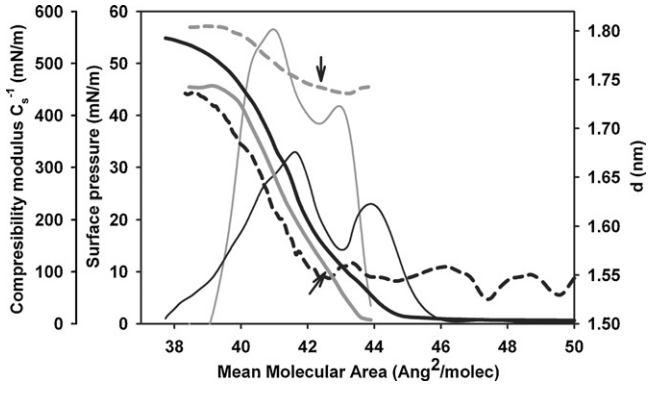

Fig. 6. BAM measurement of film thickness of pCer phases. Compression isotherms (thick full lines), film thickness "d" (dashed line) and compressibility modulus C_s^{-1} (thin line) are shown for the first compression of a monolayer at 33 °C (black) and the second compression of a monolayer at 22 °C (gray). The arrows indicate the liquid-condensed–solid phase transition for the 22 °C experiment. The curves show a single representative experiment from a set of duplicates.

Our results are summarized in Fig. 7a. The two-dimensional phase diagram of pCer monolayers shows the presence of two condensed phases and a liquid-expanded phase. The threshold pressure point for monolayer stability (collapse point) is also shown. At low temperatures pCer is present as a solid phase with highly condensed clusters and high resistance to boundary deformation. This resistance could be measured form the excess free energy of compression required to first compress a monolayer formed at 0 mN/m, compared to the second compression (Fig. 2b). The first and second compressed films become indistinguishable at certain surface pressure: the lower the temperature the higher surface pressure required for this. Such observation is included in the phase diagram where a coexistence (S + gas) phase area can be delimited (Fig. 7a and b). An increase of temperature induces a diffuse [probably second order (Albrecht et al., 1978; Atkins, 1990)] phase transition to a LC phase. This transition, although reproducible, is observed from isotherms over a small range of temperatures around room temperature. BAM observation of pCer monolayers shows a uniform increase in reflectivity when changing form LC to S phase (see Fig. 6) without evidence for the existence of domains (phase coexistence). The increase of reflectance indicates a discrete increase of film thickness (1.73–1.80 nm) supporting that the LC phase may be tilted. Even though this does not rule out the possibility of a coexistence phase region with domains below the resolution limit, it supports a second order character for the S → LC phase transition. Bulk pCer studies reported an untilted → tilted gel phase transition at 64 °C, notably approx. 40 °C higher than the S → LC transition in monolayers (20–25 °C), this transition in bulk showed a slow kinetics under cooling, with a direct fluid-untilted gel transition at high cooling rates (Shah et al., 1995). In our study, the transition observed from isobars and isotherms do not show complete coincidence in the phase diagram (Fig. 7a). This may be due to a slow-kinetic character of the phase transition, considering that isotherms report the LC → S transition while isobars involve S → LC transition. At room temperature, and very low surface pressure, a small three-phase coexistence region is found for gas + LC + LE phases (Fig. 7a and c). At higher temperatures a first order transition to a LE phase is observed showing a large LC + LE coexistence region (Fig. 7a and d). This transition involves a large area change (77% increase al 10 mN/m; see Figs. 1 and 5) and a decrease of the monolayer thickness (1.5 nm) (see also Fig. 6). In comparison with the tilted gel → chain-melted phase transition described in bulk studies at about 90 °C (Shah et al., 1995), the temperature range where the LC → LE phase transition takes place in monolayers is considerable lower. At 30 mN/m we found LC + LE phase coexistence at temperatures above 54 °C. If a decrease of the surface pressure to about 15 mM/m should occur at the interface [a situation easily occurring by lateral pressure fluctuations due to thermal energy, even for relatively condensed films (Phillips et al., 1975)], LC + LE phase coexistence might be present at physiological temperature (Fig. 7). Pure Cer systems lead to an hexagonal inverse structure for the chain-melted phase of Cer (Goni and Alonso, 2006).

Please cite this article in press as: Fanani, M.L., Maggio, B., Phase state and surface topography of palmitoyl-ceramide monolayers. Chem. Phys. Lipids (2010), doi:10.1016/j.chemphyslip.2010.04.008

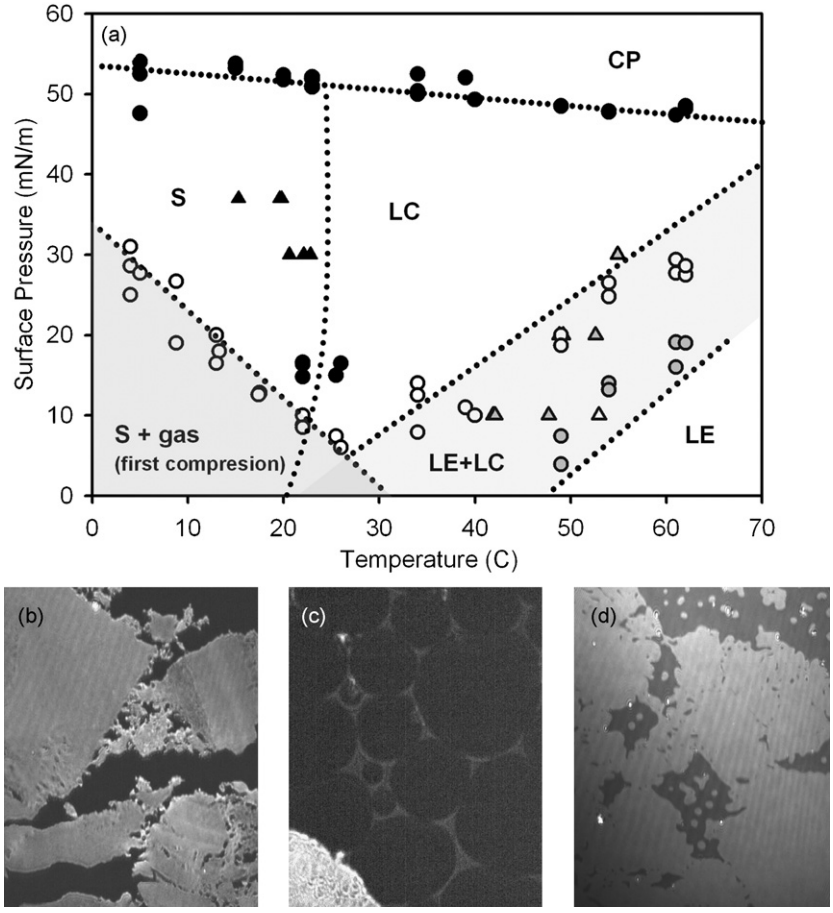

Fig. 7. Phase diagram for pCer monolayers. (a) Surface pressure vs. temperature phase diagram of pCer from isotherms (circles) and isobars (triangles) data. A solid (S), a liquid-condensed (LC) and a liquid expanded (LE) phase are identified in the temperature and pressure range explored. Additionally, the collapse point of each isotherm provides information of the transition to the collapsed phase (CP). Black symbols correspond to second order transitions, gray and white symbols correspond to the beginning and the end of first order transitions respectively. The gray shadowed areas indicate phase coexistence regions: the bottom left triangle indicates gas–solid coexistence only for the first compression of the monolayer as illustrated in (b); the small triangle in the bottom centre is a three phase (LC/LE/gas) coexistence region as illustrated in (c); and the shadowed area on the right corresponds to a LC–LE coexistence region as illustrated in (d). Image size 372 μm × 466 μm. The data in (a) correspond to the whole set of experiments where each point corresponds to a single experiment. The images are representative experiments.

In the present study we provided information on the lateral structural behavior of pCer constrained to a planar interface. This may allow direct comparisons with the behavior of Cer when included in lipid domains formed in regions of relatively low curvature of bilayer membranes.

4. Conclusions

In this work we advanced understanding of the phase behavior of pCer restricted to a planar interface using Langmuir monolayers under strictly controlled and known surface packing conditions. The results indicate that pCer can exhibit expanded, as well as condensed phase states. Formation of three phases was found, depending on the surface pressure and temperature: a solid (1.80 nm thick), a liquid-condensed (1.73 nm thick, likely tilted) and a liquid-expanded (1.54 nm thick) phase over the temperature range 5–62 °C. A large hysteretic behavior is observed for the S phase monolayer that can be due to its high resistance to domain boundary deformation. A second (or higher) order S → LC phase transition is observed at about room temperature while a first order LC → LE transition occurs in a range of temperature encompassing the physiological one (observed from 30 °C at low surface pressure). This phase behavior broadens the view of Cer as a type of lipid not-always-rigid but able to exhibit polymorphic properties.

Acknowledgements

This work was supported by SECyT-UNC, ACC-MinCyT (Prov. Córdoba), CONICET and FONCyT (Argentina); some aspects of this investigation are inscribed within the PAE 22642 network in Nanobiosciences. B.M. and M.L.F. are Career Investigators of CONICET.

References

Albrecht, O., Gruler, H., Sackmann, E., 1978. Polymorphism of phospholipid monolayers. Le Journal De Physique 39, 301–313.
Ali, S., Brockman, H.L., Brown, R.E., 1991. Structural determinants of miscibility in surface films of galactosylceramide and phosphatidylcholine: effect of unsaturation in the galactosylceramide acyl chain. Biochemistry 30, 11198–11205.
Atkins, P.W., 1990. Physical Chemistry, fourth ed. Freeman W.H., New York.
Bianco, I.D., Maggio, B., 1989. Interactions of neutral and anionic glycosphingolipids with dilauroylphosphatidylcholine and dilauroylphosphatidic acid in mixed monolayers. Colloids Surf. 40, 249–260.
Brockman, H.L., Jones, C.M., Schwebke, C.J., Smaby, J.M., Jarvis, D.E., 1980. Application of microcomputer-controlled film balance system to collection and analysis of data from mixed monolayers. J. Colloid Interface Sci. 78, 502–512.
Busto, J.V., Fanani, M.L., De, T.L., Sot, J., Maggio, B., Goni, F.M., Alonso, A., 2009. Coexistence of immiscible mixtures of palmitoylsphingomyelin and palmitoylceramide in monolayers and bilayers. Biophys. J. 97, 2717–2726.
Carrer, D.C., Maggio, B., 1999. Phase behavior and molecular interactions in mixtures of ceramide with dipalmitoylphosphatidylcholine. J. Lipid Res. 40, 1978–1989.
Chen, H., Mendelsohn, R., Rerek, M.E., Moore, D.J., 2000. Fourier transform infrared spectroscopy and differential scanning calorimetry studies of fatty acid homogeneous ceramide 2. Biochim. Biophys. Acta 1468, 293–303.

Please cite this article in press as: Fanani, M.L., Maggio, B., Phase state and surface topography of palmitoyl-ceramide monolayers. Chem. Phys. Lipids (2010), doi:10.1016/j.chemphyslip.2010.04.008

Davies, J.T., Rideal, E.K., 1963. Interfacial Phenomena. Academic Press, NY.
Ducharme, D., Max, J.J., Salesse, C., Leblanc, R.M., 1990. Ellipsometric study of the physical states of phosphatidylcholine at the air–water interface. J. Phys. Chem. 94, 1925–1932.
Estep, T.N., Mountcastle, D.B., Barenholz, Y., Biltonen, R.L., Thompson, T.E., 1979. Thermal behavior of synthetic sphingomyelin–cholesterol dispersions. Biochemistry 18, 2112–2117.
Fanani, M.L., Hartel, S., Maggio, B., De, T.L., Jara, J., Olmos, F., Oliveira, R.G., 2010. The action of sphingomyelinase in lipid monolayers as revealed by microscopic image analysis. Biochim. Biophys. Acta, Epub ahead of print Jan 11.
Fidelio, G.D., Maggio, B., Cumar, F.A., 1986. Molecular parameters and physical state of neutral glycosphingolipids and gangliosides in monolayers at different temperatures. Biochim. Biophys. Acta 854, 231–239.
Goni, F.M., Alonso, A., 2006. Biophysics of sphingolipids I. Membrane properties of sphingosine, ceramides and other simple sphingolipids. Biochim. Biophys. Acta 1758, 1902–1921.
Goni, F.M., Alonso, A., 2009. Effects of ceramide and other simple sphingolipids on membrane lateral structure. Biochim. Biophys. Acta 1788, 169–177.
Grassme, H., Riethmuller, J., Gulbins, E., 2007. Biological aspects of ceramide-enriched membrane domains. Prog. Lipid Res. 46, 161–170.
Holopainen, J.M., Brockman, H.L., Brown, R.E., Kinnunen, P.K., 2001. Interfacial interactions of ceramide with dimyristoylphosphatidylcholine: impact of the N-acyl chain. Biophys. J. 80, 765–775.
Holopainen, J.M., Lemmich, J., Richter, F., Mouritsen, O.G., Rapp, G., Kinnunen, P.K., 2000. Dimyristoylphosphatidylcholine/C16:0-ceramide binary liposomes studied by differential scanning calorimetry and wide- and small-angle X-ray scattering. Biophys. J. 78, 2459–2469.
Karttunen, M., Haataja, M.P., Saily, M., Vattulainen, I., Holopainen, J.M., 2009. Lipid domain morphologies in phosphatidylcholine-ceramide monolayers. Langmuir 25, 4595–4600.
Kolesnick, R.N., Goni, F.M., Alonso, A., 2000. Compartmentalization of ceramide signaling: physical foundations and biological effects. J. Cell Physiol. 184, 285–300.
Kooijman, E.E., Vaknin, D., Bu, W., Joshi, L., Kang, S.W., Gericke, A., Mann, E.K., Kumar, S., 2009. Structure of ceramide-1-phosphate at the air–water solution interface in the absence and presence of Ca^{2+}. Biophys. J. 96, 2204–2215.
Lheveder, C., Meunier, J., Henon, S., 2000. Brewster angle microscopy. In: Baszkin, A., Norde, W. (Eds.), Physical Chemistry of Biological Interfaces. Marcel Dekker, Inc., NY.
Lopez-Montero, I., Monroy, F., Velez, M., Devaux, P.F., 2009. Ceramide: from lateral segregation to mechanical stress. Biochim. Biophys. Acta.
Maggio, B., 2004. Favorable and unfavorable lateral interactions of ceramide, neutral glycosphingolipids and gangliosides in mixed monolayers. Chem. Phys. Lipids 132, 209–224.
Maggio, B., Carrer, D.C., Fanani, M.L., Oliveira, R.G., Rosetti, C.M., 2004. Interfacial behavior of glycosphingolipids and related sphingolipids. Curr. Opin. Colloid Interface Sci. 8, 448–458.
Maggio, B., Cumar, F.A., Caputto, R., 1978. Interactions of gangliosides with phospholipids and glycosphingolipids in mixed monolayers. Biochem. J. 175, 1113–1118.
Mohwald, H., 1995. Phospholipids monolayers. In: Lipowsky, R., Sackmann, E. (Eds.), Structure and Dynamics of Membranes. Elsevier, Amsterdam, pp. 161–211.
Phillips, M.C., Graham, D.E., Hauser, H., 1975. Lateral compressibility and penetration into phospholipid monolayers and bilayer membranes. Nature 254, 154–156.
Rosetti, C.M., Oliveira, R.G., Maggio, B., 2003. Reflectance and topography of glycosphingolipid monolayers at the air-water interface. Langmuir 19, 377–384.
Shah, J., Atienza, J.M., Duclos Jr., R.I., Rawlings, A.V., Dong, Z., Shipley, G.G., 1995. Structural and thermotropic properties of synthetic C16:0 (palmitoyl) ceramide: effect of hydration. J. Lipid Res. 36, 1936–1944.
Smaby, J.M., Kulkarni, V.S., Momsen, M., Brown, R.E., 1996. The interfacial elastic packing interactions of galactosylceramides, sphingomyelins, and phosphatidylcholines. Biophys. J. 70, 868–877.
Smaby, J.M., Momsen, M.M., Brockman, H.L., Brown, R.E., 1997. Phosphatidylcholine acyl unsaturation modulates the decrease in interfacial elasticity induced by cholesterol. Biophys. J. 73, 1492–1505.
van Blitterswijk, W.J., van der Luit, A.H., Veldman, R.J., Verheij, M., Borst, J., 2003. Ceramide: second messenger or modulator of membrane structure and dynamics? Biochem. J. 369, 199–211.
Veiga, M.P., Arrondo, J.L., Goni, F.M., Alonso, A., 1999. Ceramides in phospholipid membranes: effects on bilayer stability and transition to nonlamellar phases. Biophys. J. 76, 342–350.
Venien, C., Le, G.C., 1988. Phospholipid asymmetry in renal brush-border membranes. Biochim. Biophys. Acta 942, 159–168.

Please cite this article in press as: Fanani, M.L., Maggio, B., Phase state and surface topography of palmitoyl-ceramide monolayers. Chem. Phys. Lipids (2010), doi:10.1016/j.chemphyslip.2010.04.008